

REMOVAL OF IMPULSE BURSTS IN RADAR IMAGES

Pertti T. Koivisto[†], Vladimir V. Lukin[‡], Vladimir P. Melnik[‡], Oleg V. Tsymbal[‡]

[†]Signal Processing Laboratory, Tampere University of Technology
P.O.Box-553, FIN-33101, Tampere, FINLAND, Tel. +358 3 365 3860,
Fax +358 3 365 3857, E-mail: peko@cs.tut.fi, melnik@cs.tut.fi

[‡]Dept 504, State Aerospace University (Kharkov Aviation Institute)
17 Chkalova Street, 61070, Kharkov, UKRAINE,
Tel/fax + 38 0572 441186, E-mail: lukin@mmds.kharkov.ua

ABSTRACT

The characteristics of impulse bursts in radar images are analyzed and methods for the removal of the bursts are discussed. As a case study, soft morphological filters utilizing a training-based optimization scheme are used for the noise removal. It is shown that the methods used can provide an effective removal of impulse bursts even if two neighboring rows of an image are corrupted. At the same time the multiplicative noise in images is also suppressed together with good edge and detail preservation. Numerical simulation results as well as examples of real radar images are presented.

1. INTRODUCTION

Remote sensing radar images are usually formed on board of an aircraft or spaceborne carrier where a radar antenna and primary signal processing devices are installed [1]. Then, the formed image is usually transferred to one or few on-land remote sensing data processing centers, where the image is subject to visualization, analysis, filtering, interpretation, etc. For transferring the remote sensing data, the standard or special communication channels are used and, since images are often encoded and then decoded, impulsive noise may be observed in images [2, 3].

In many practical situations the probability of spikes is low and two or more neighboring pixels are very seldom corrupted by impulsive noise. In other words, the spikes possess approximately spatially invariant characteristic [3]. Many efficient and robust filtering algorithms have been already proposed to remove spikes that fulfill the aforementioned model assumptions [3-5]. However, these assumptions are not valid in some practical situations.

In particular, the interference can be long term and so intensive that it corrupts several consecutive image pixels in one or more rows following each other. Such situations may happen, e.g., if the receiver input and circuitry are not well protected against intensive interference or if in the neighborhood of the remote sensing data processing center there are some electromagnetic

wave irradiation sources operating in the frequency band which overlaps with communication channel wave band. Real life illustrations of what happens in this case with radar images are presented below. (In this paper, we assume that images are transferred rowwise. Naturally, similar methods can also be applied if images are transferred columnwise.)

In paper [6], Koivisto *et. al.* have shown that training-based optimized soft morphological filters are able to remove line-type noise well enough. For example, the obtained filters could remove line-type noise with horizontal or almost horizontal orientations. As this noise in a certain sense corresponds to the impulse bursts that we have in the considered case, it is reasonable to expect that soft morphological filters being trained for the removal of impulse bursts are able to perform well for radar image recovery.

However, there are also some differences between the task considered here and the design task studied in the reference [6]. First, the impulse bursts differ from the line-type noise since the former one has more complicated and random behavior. Second, the radar images are characterized by the presence of multiplicative noise. Hence, the training task is now much more complicated.

In this paper, we analyze the properties of impulse bursts in radar images and propose a model for this noise. The model also takes into consideration the multiplicative noise present in radar images. This model is then used in the training and optimization of soft morphological filters. Different approaches for the training are discussed. The test data and real radar image examples are presented.

2. PROPERTIES AND MODEL OF IMPULSE BURSTS IN RADAR IMAGES

To get an idea what the impulse bursts are, let us first analyze a radar image that was received by the Center of Earth Remote Sensing (Kharkov, Ukraine) via telecommunication channel from Ukrainian satellite "Sich-1." A 256x219 part of the radar image is presented in Fig. 1a. It can be seen that several fragments

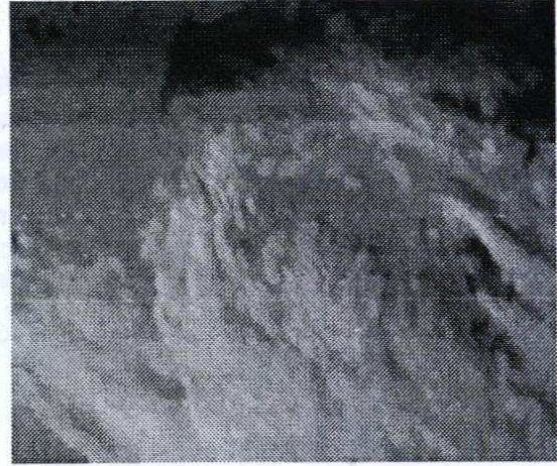
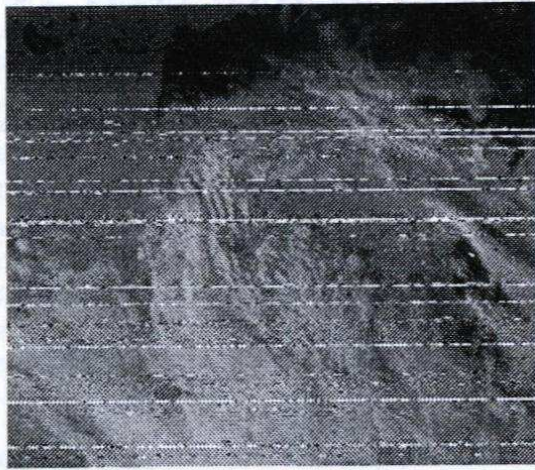


Fig. 1. (a) A part of the original radar image and (b) the part filtered by the proposed soft morphological filter (see text).

in many rows are corrupted by impulse bursts, and the lengths of such fragments are rather different. Moreover, sometimes such fragments occur in two consecutive rows. It can also be observed visually that in some pixels of the considered fragments the values are maximal (i.e., 255 in the 8-bit representation used) while some pixel values differ from 255 but still remain "impulsive" with respect to the values that can be predicted for the radar image from its local analysis.

As we use training-based design method, we need a corrupted and a true (desired) training image. Since it is impossible to have such uncorrupted real radar image, artificial test images must be used.

In order to make an adequate model of a test radar image, we studied the properties of the real image in more details. First, the percentage of pixels corrupted by impulse bursts was calculated. The percentage was approximately 5%. Then, the statistical characteristics of burst lengths were estimated. Finally, the behavior of the bursts was studied row by row for the rows containing bursts. It was found that the mean of the burst fragment values was approximately 180, the bursts contained a quasisinusoidal component and a noisy component. Besides, cut-off effects were observed, that is, there may be several pixels in a row having values equal to 255. The multiplicative noise is also present in the real radar image. The probability density function of this noise is Gaussian with 1 as the mean. The evaluated relative variance is approximately 0.05.

All aforementioned properties of the impulse bursts and the multiplicative noise have been taken into account when generating the noise model for the test image. Since images are transferred as one-dimensional arrays the noise model is also presented for one-dimensional array. More precisely, our noise model is now the following.

First, a Markov-chain with two states is used to determine which samples belong to impulse bursts. The

transition probability from "no-burst-state" to "burst-state" is p and the transition probability from "burst-state" to "no-burst-state" is q .

If a sample does not belong to an impulse burst then it is corrupted by the aforementioned multiplicative noise in the usual way. On the other hand, if a sample belongs to an impulse burst then the (corrupted) sample value f_j is obtained using the formula

$$f_j = \text{round}\{\alpha + \beta \sin[(j-k)\omega + \varphi_k] + \xi_j\},$$

where k denotes the index of the leftmost sample in the burst in question, α is the average level of impulsive noise, β and ω are the amplitude and frequency of the harmonic component of the burst, respectively, φ_k denotes the phase of the harmonic component of the burst, and ξ_j is the fluctuating noise component of the burst. The phase $\varphi_k \in]-\pi, \pi]$ is a random variable with uniform distribution and the noise component ξ_j is a random variable with Gaussian probability density function with zero mean and standard deviation σ . Hence, α , β , and ω are common to all bursts, φ_k is common to all pixels in some burst, and ξ_j varies from pixel to pixel. Rounding is to the nearest non-negative integer less than or equal to 255.

A test image of size 256x256 corrupted by multiplicative noise and impulse burst is presented in Fig. 2a. The estimated parameter values for the noise model were $p = 0.9993$, $q = 0.989$, $\alpha = 200$, $\beta = 80$, $\omega = 0.7$, and $\sigma = 30$. Then, the percentage of the pixels belonging to the bursts was approximately 5%. The test image contains homogeneous regions, large size objects with different shapes, and small size objects also having different shapes, contrasts and orientations. Besides this noisy test image, we used a noise free test image, a test image corrupted by multiplicative noise only, a test image corrupted by impulse bursts only, and a test image corrupted by impulse burst and negative impulsive noise (i.e., here spikes with amplitude 0). Those test images

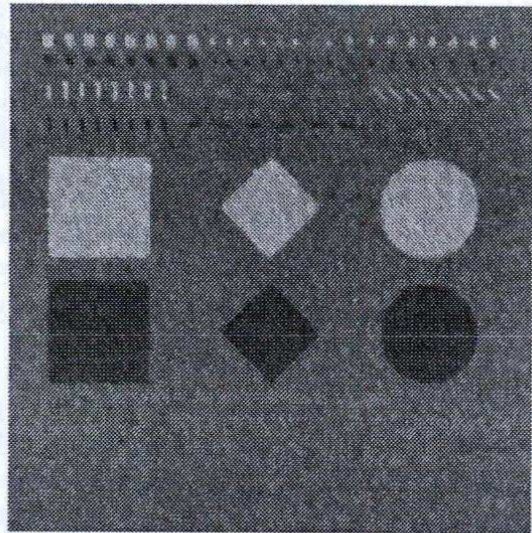
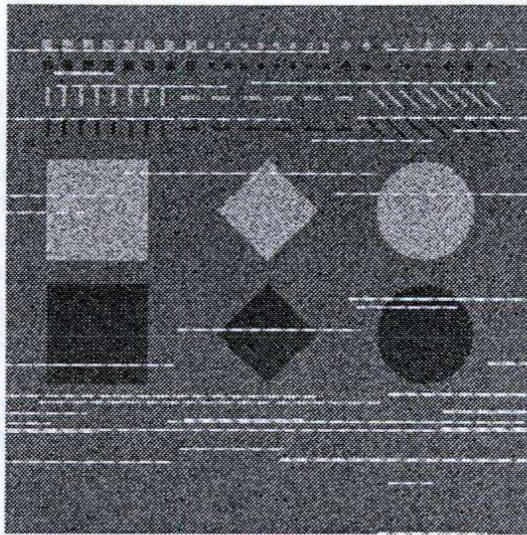


Fig. 2. (a) Original test image with multiplicative noise and impulse bursts and (b) its filtered counterpart (see text).

were needed to study different approaches to the training of the soft morphological filters (see Section 4).

Our desire was also to check whether the soft morphological filters destroy many details while removing the impulse bursts. By comparing the images in Fig. 1a and Fig. 2a, one can see that the structure and general properties of the images are similar enough also for this purpose.

3. SOFT MORPHOLOGICAL FILTERS

Soft morphological filters [7] form a class of stack filters and were introduced to improve the behavior of standard flat morphological filters in noisy conditions. They have many desirable properties, e.g., they can be designed to preserve details well [8]. In addition, they are suitable for impulsive or heavy-tailed noise.

The two basic soft morphological operations are *soft erosion* and *soft dilation*. Based on these operations, two compound operations, *soft opening* and *soft closing*, can be defined in the usual way. As we consider in this paper images only, the definitions are also given in two-dimensional signal space.

Definition 1. The *structuring system* $[B, A, r]$ consists of three parameters, finite sets A and B , $A \subseteq B \neq \emptyset$, in \mathbf{Z}^2 and an integer r satisfying $1 \leq r \leq \max\{1, |B \setminus A|\}$. The set B is called the *structuring set*, A its (hard) *center*, $B \setminus A$ its (soft) *boundary*, and r the *order index* of its center or the *repetition parameter*.

The *translated set* T_x , where the set T is translated by x , $x \in \mathbf{Z}^2$, is defined by $T_x = \{x+t : t \in T\}$. A *multiset* is a collection of objects, where the repetition of objects is allowed. For example, $\{1, 1, 1, 2, 3, 3\} = \{3 \diamond 1, 2 \diamond 2, 3 \diamond 3\}$ is a multiset.

Soft morphological operations transform a signal $f: \mathbf{Z}^2 \rightarrow \mathbf{R}$ to another signal by the following rules.

Definition 2. The *soft erosion (soft dilation)* of f by the structuring system $[B, A, r]$ is denoted by $f \ominus [B, A, r]$ ($f \oplus [B, A, r]$), where $f \ominus [B, A, r](t)$ ($f \oplus [B, A, r](t)$) is the r 'th smallest (largest) value of the multiset $\{r \diamond f(a) : a \in A_i\} \cup \{f(b) : b \in (B \setminus A)_i\}$.

A *finite composition* of length p of basic soft morphological operations is simply a sequence of p soft erosions and/or dilations, where each operation can have different structuring system. Naturally, each operation is applied to the result of the previous operation in the sequence.

4. OPTIMIZATION

Although there are no analytical criteria for deciding which soft morphological operation (and with which parameters) is the best for some situation, a suitable operation sequence and its parameters can be found using supervised learning methods, e.g., simulated annealing and genetic algorithms [6]. Of course, some training set, for which the desired output is known, is needed.

The optimization methods presented in [6] allow one to handle the impulse bursts in several ways. First, it is possible to search the optimal filter using the noise-free test image as the target image and the image corrupted by impulse bursts and multiplicative (or negative impulsive) noise as the source image.

Another possibility is to use structural constraints, in which case the target image is the noise-free image and the source image is the image corrupted by multiplicative noise. The impulse bursts are presented as constraints and the optimal filter is sought, provided that the impulse bursts are removed (totally or at least to some extent).

A third possibility is to optimize the soft morphological operations to remove impulse bursts only. Then, at the second stage, the multiplicative noise can be sup-

pressed by some conventional technique suited for this purpose [4, 5]. In this case the target image is the image corrupted by multiplicative noise and the source image is the image corrupted by impulse bursts and multiplicative noise. However, this third possibility is not studied in this paper but it is left as a topic for future research.

As the error criterion, it is possible to use any criterion that can be calculated using two images as parameters. In this paper, we have used the *mean absolute error* (MAE) and the *mean square error* (MSE).

5. EXPERIMENTAL RESULTS

The experimental tests in this paper are based on the following test case. The training image pairs are the ones discussed in Sections 2 and 4. The application image is the one shown in Fig. 1a. In each case the optimal composite soft operation of length 2 were sought with overall dimensions 3x3, 3x5 (i.e., 3 columns and 5 rows), and 5x5 (i.e., the structuring sets were inside the 3x3, 3x5, and 5x5 rectangles). The length two was selected since now our noisy image contains both positive and negative impulsive noise and a single soft operation is not able to remove two-sided noise. On the other hand, as the experiments showed, two consecutive soft operations are already powerful enough for our purposes.

When the 3x3 window was used, the optimal filters were not able to remove impulse bursts sufficiently. On the other hand, the filters optimal inside the 3x5 and 5x5 windows were already able to remove almost all of the bursts. Hence, the quality of these filters depended on their ability to remove multiplicative noise and preserve details.

The optimal filter sequence was usually soft erosion followed by soft dilation. This is also natural since the noise was mostly positive. However, the results achieved by the optimal soft openings (i.e., the soft erosion followed by the soft dilation with the symmetric structuring set) were usually almost as good as those achieved with the optimal composite soft operations of length 2. This is important since the optimization of soft openings is much easier than the optimization of composite soft operations of length 2.

The error criterion used (i.e., the MAE or the MSE) did not seem to have crucial effect in the optimization. However, the filters optimized under the MSE produced visually better results although, in general, the differences were small.

When comparing the optimization schemes, we noticed that visually the best results were achieved with the noise-free test image as the target image and the image corrupted by impulse bursts and multiplicative (or negative impulsive) noise as the source image. The results obtained using structural constraints were not as good but, however, of good quality. Moreover, there did not seem to be much difference between the cases in

which multiplicative or negative impulsive noise was used together with impulse bursts.

As an example of the results of the method, Fig. 1b and Fig. 2b show two images that are filtered by the found optimal filters (the same filter sequence in both cases). The optimal filter sequence is soft erosion followed by soft dilation and the sequence was found under the MSE and inside the 3x5 window. The target image was the noise-free test image and the source image was the test image corrupted by impulse bursts and multiplicative noise (i.e., the image in Fig. 2a). As can be seen, the image in Fig. 2b is a little blurred and some small, especially horizontal, details are lost. However, all impulse bursts are removed. The same also holds for the radar image in Fig. 1b; impulse bursts have disappeared and small distortion has appeared.

6. CONCLUSION

The characteristics of impulse bursts in radar images were analyzed and a method for the removal of the bursts was discussed. It was shown through experiments that the presented method can remove impulse bursts and multiplicative noise with efficiency and at the same time preserve details well. Although our test case was quite limited the method can easily be applied to other cases as well.

REFERENCES

- [1] *Remote Sensing Digital Image Analysis. An Introduction*, Edited by J.A. Richards, Springer Verlag, Berlin, 1994.
- [2] K.-H. Szekiolda, *Satellite Monitoring of the Earth*, Wiley, New York, 1989.
- [3] J. Astola and P. Kuosmanen, *Fundamentals of Nonlinear Digital Filtering*, CRC Press, Boca Raton, Florida, 1997.
- [4] I. Pitas and A.N. Venetsanopoulos, *Nonlinear Digital Filters: Principles and Applications*, Kluwer Academic Publishers, Boston, 1990.
- [5] V.P. Melnik, *Nonlinear Locally Adaptive Techniques for Image Filtering and Restoration in Mixed Noise Environment*, Dr. Tech. Thesis, Tampere University of Technology, Tampere, Finland, March 2000.
- [6] P. Koivisto, H. Huttunen, and P. Kuosmanen, "Training Based Optimization of Soft Morphological Filters," *Journal of Electronic Imaging*, vol. 5, pp. 300-322, June 1996.
- [7] L. Koskinen and J. Astola, "Soft morphological filters: A robust morphological filtering method," *Journal of Electronic Imaging*, vol. 3, pp. 60-70, January 1994.
- [8] P. Kuosmanen and J. Astola, "Soft morphological filtering," *Journal of Mathematical Imaging and Vision*, vol. 5, pp. 231-262, September 1995.